Supporting Information

Inhibition of shuttle effect of lithium-sulfur battery by tannic acid-metal in-situ chemical film-forming modified separator

Liwen Yang[a], Yang Wang[a], Qian Li[a], Yuan Li[a], Yanxiao Chen[a, *],Yuxia Liu[b], Zhenguo Wu[a], Gongke Wang[c], Benhe Zhong[a], Yang Song[a], Wei Xiang[d], Yanjun Zhong[a], Xiaodong Guo[a]

[a] School of Chemical Engineering, Sichuan University, No. 24 South Section 1, Yihuan Road, Chengdu, 610065, PR China

[b] The Key Laboratory of Life-Organic Analysis, Key Laboratory of Pharmaceutical Intermediates and Analysis of Natural Medicine, School of Chemistry and Chemical Engineering, Qufu Normal University, Qufu, 273165, Shandong, PR China

[c] School of Materials Science and Engineering, Henan Normal University, XinXiang, 453007，PR China.

[d] College of Materials and Chemistry &Chemical Engineering, Chengdu University of Technology, Chengdu, 610059, PR China.

[*] Corresponding author.

E-mail address: yxchen888@163.com (Y. Chen).

Table S1. Mass loading of TA-Co

	Pristine PP separator(mg)	Coated separator(mg)	Coating mass(mg)	Mass loading(mg/cm^2)
PP	3.03	-	-	-
TA-Co	3.03	3.204	0.174	**0.055**

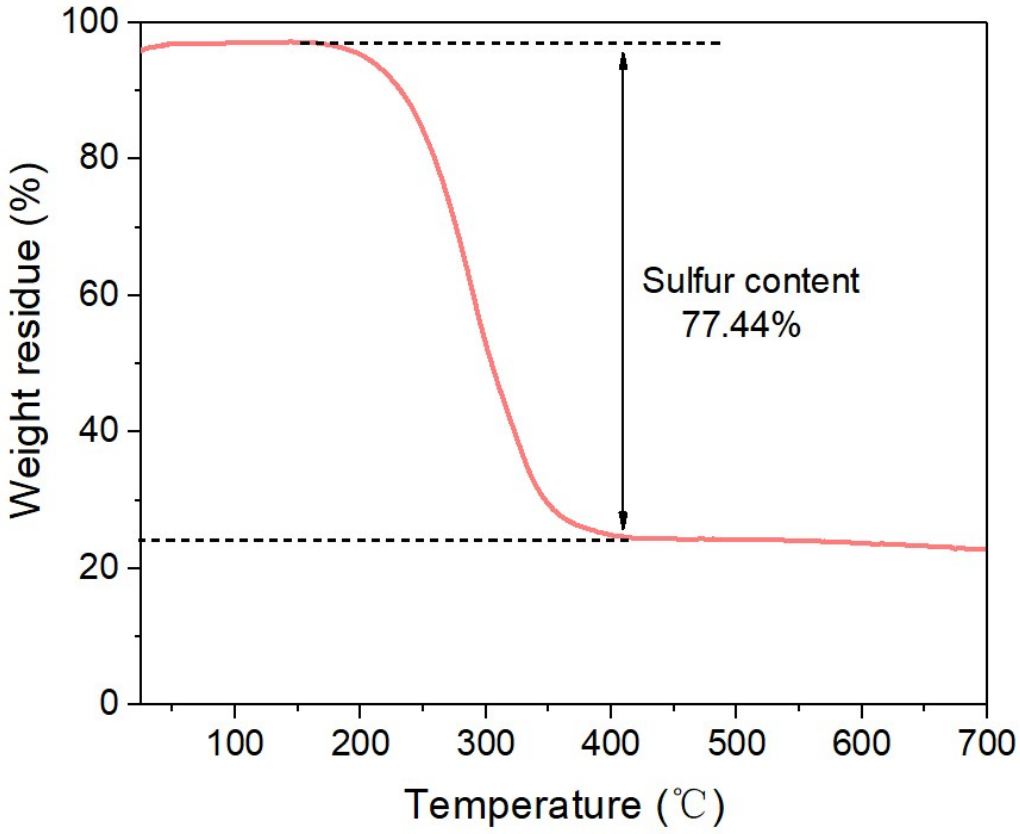

Fig S1. TGA curve of S/KB composite under N_2 atmosphere.

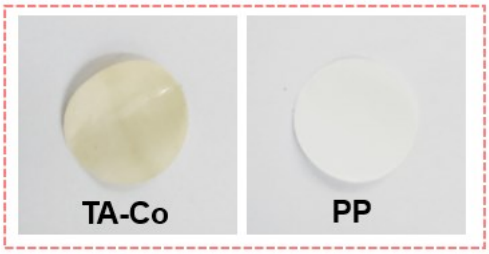

Fig S2. Optical photo of TA-Co and PP separator.

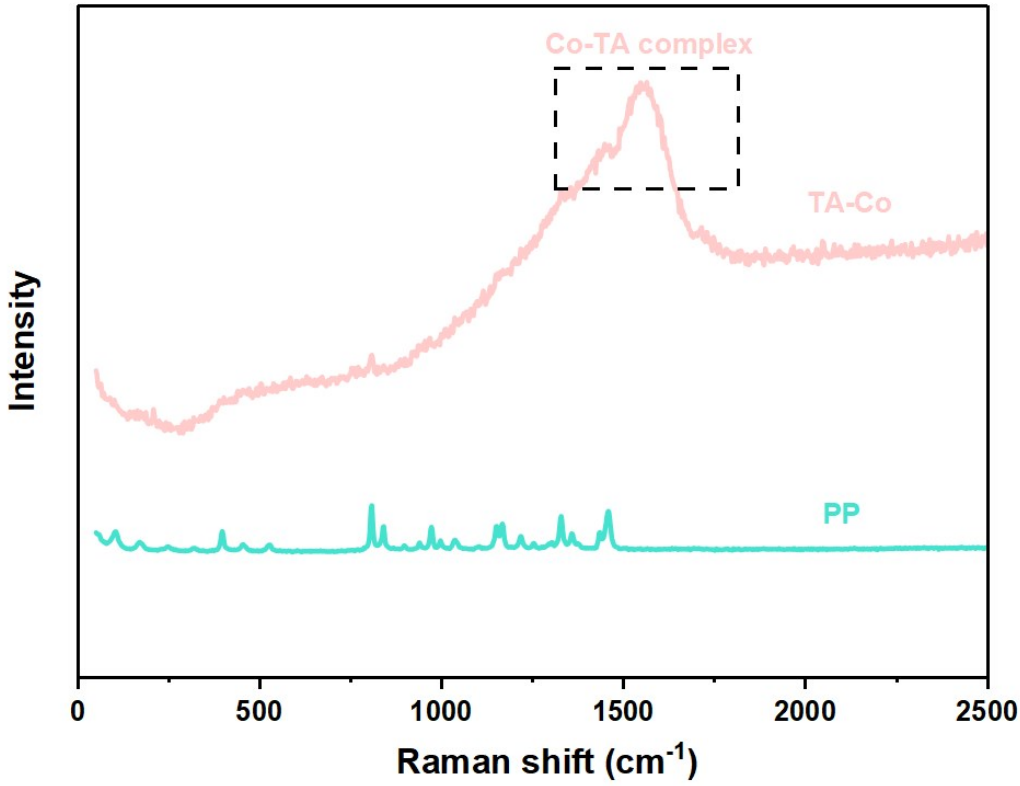

Fig S3. Raman spectra of TA-Co separator and PP separator.

Fig S4. Folding-unfolding experiment of TA-Co separator.

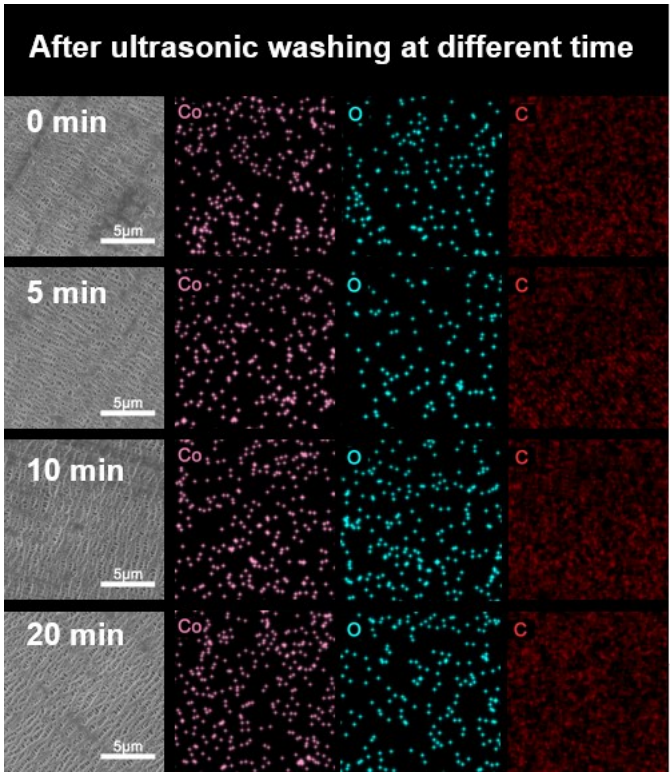

Fig S5. EDS-mapping of TA-Co separator after ultrasonic washing at different time.

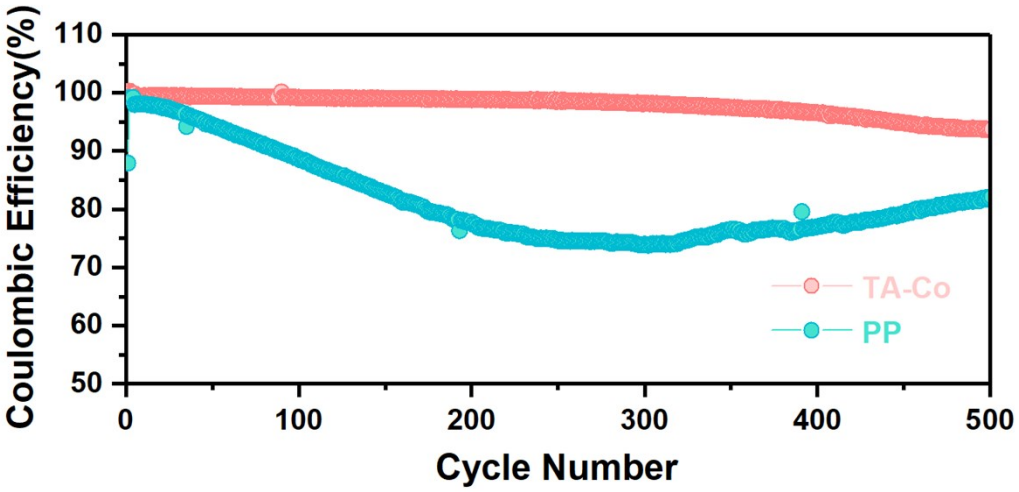

Fig S6. Coulombic efficiency of the cell of TA-Co and PP separator.

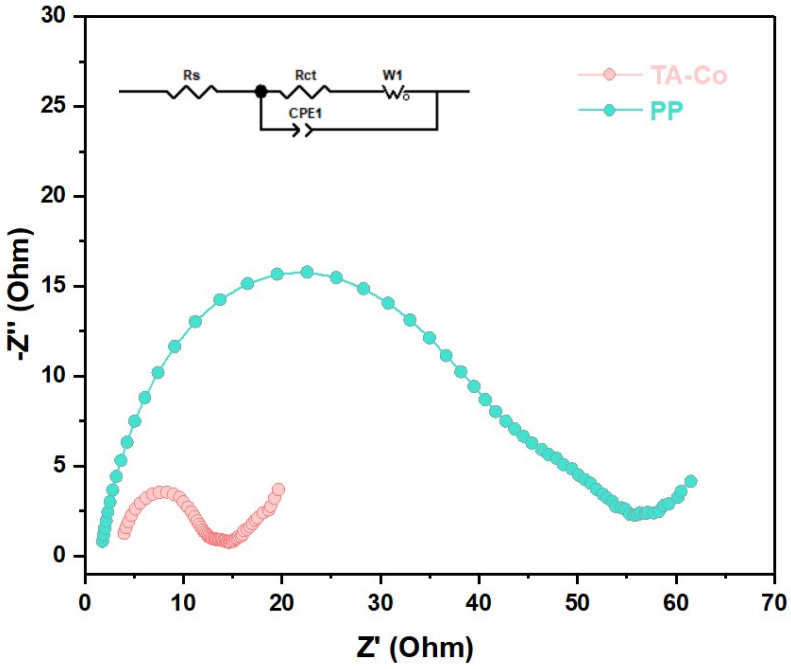

Fig S7. EIS of cells with TA-Co and PP separator before cycling.

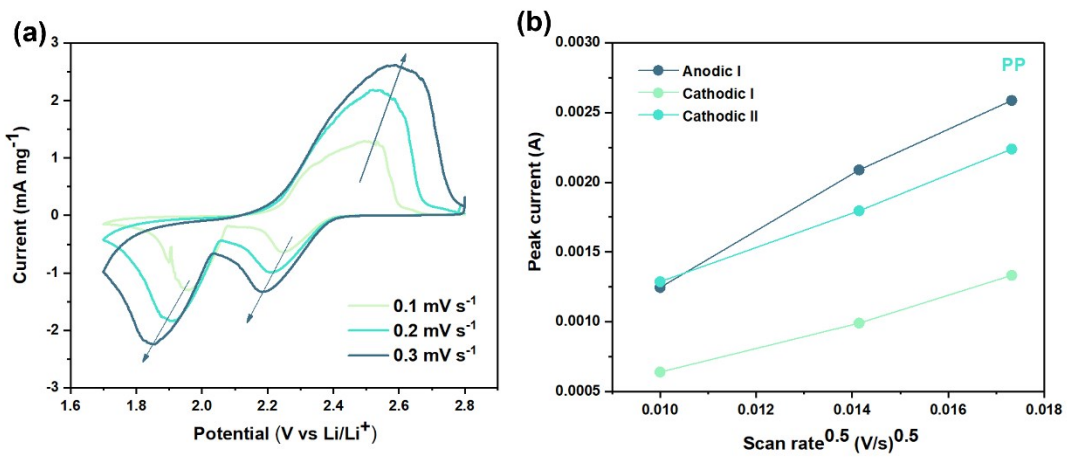

Fig S8. (a). CV curves of cells with PP separator from 0.1mV s-1 to 0.3mV s-1. (b). The linear fits of the peak currents for cells with PP separator.

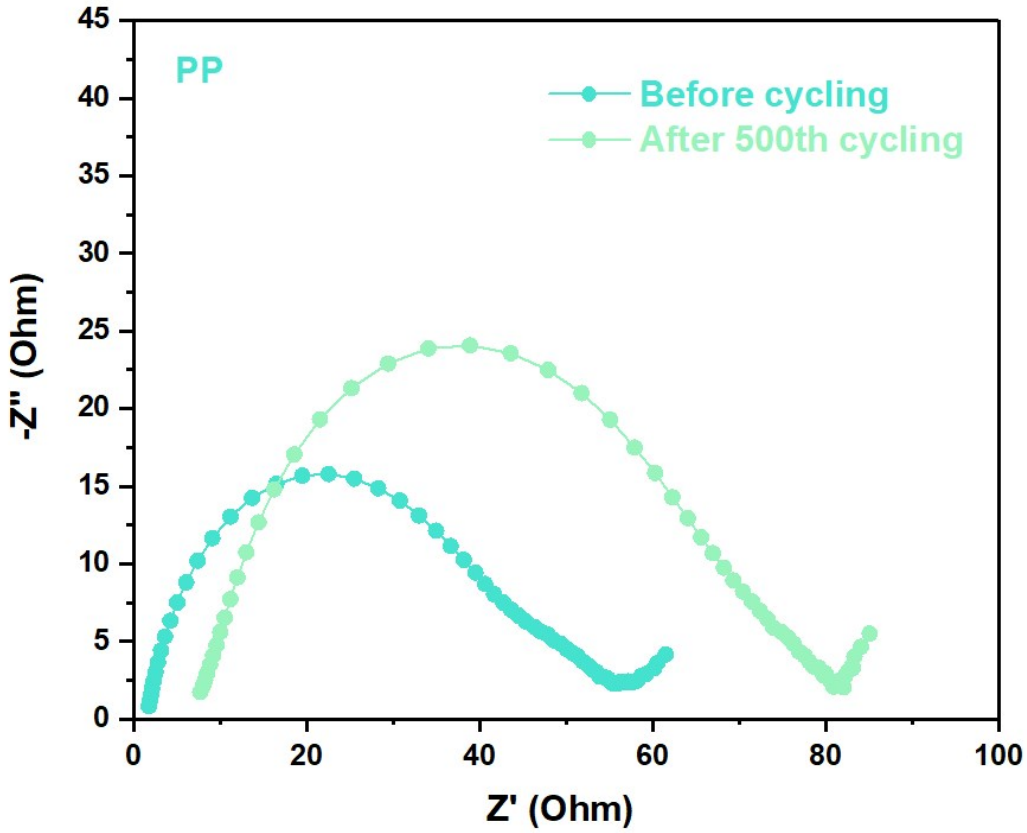

Fig S9. EIS of cells with PP separator before and after cycling.